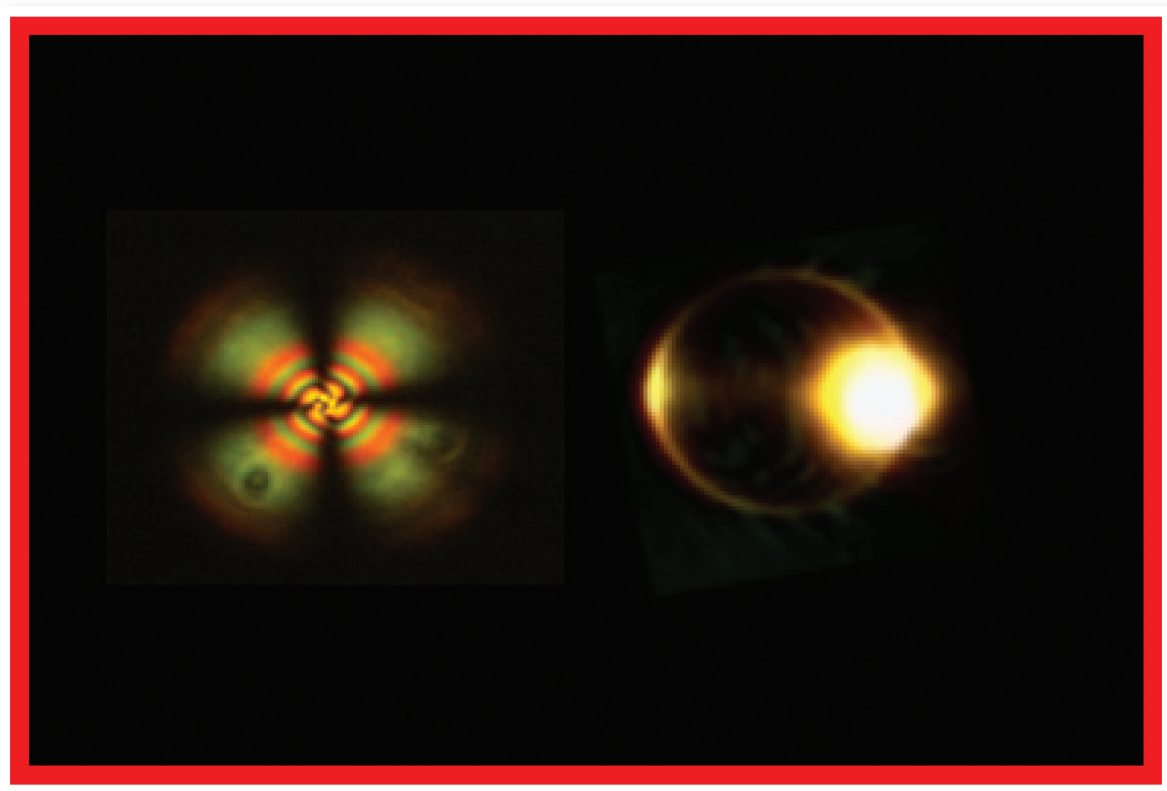


2 February 2015

Volume 106 Number 5

# AIP | Applied Physics Letters



[apl.aip.org](http://apl.aip.org)

## Detection of phase transitions from the study of whispering gallery mode resonance in liquid crystal droplets

T. Arun Kumar,<sup>a)</sup> M. A. Mohiddon, N. Dutta, Nirmal K. Viswanathan, and Surajit Dhara<sup>b)</sup>  
*School of Physics, University of Hyderabad, Hyderabad, India*

(Received 15 November 2014; accepted 14 December 2014; published online 2 February 2015)

We report studies on the whispering gallery mode (WGM) resonance of liquid crystal (LC) droplets across the smectic-A (SmA) to nematic phase transition. The quality factor (Q) in the SmA phase decreases rapidly with a characteristic slope change at the SmA-N transition. In the SmA phase, Q-factor is linearly proportional to the birefringence ( $\Delta n$ ). We discuss the effect of topological defect transformation on the WGM resonance. The study of WGM resonance is expected to be very useful for detecting subtle phase transitions among LC mesophases. © 2015 AIP Publishing LLC. [<http://dx.doi.org/10.1063/1.4906615>]

Optical microresonators are very important from both the technological and fundamental points of view. Because of their small mode volume and high Q-factors optical microresonators are widely used as laser sources, active filters, and all-optical switches.<sup>1</sup> The high Q associated with the resonant modes in the microresonators has inspired various experiments. For example, the high energy density in the cavities facilitate the observation of various low threshold nonlinear processes such as switching of coherent light, low-threshold lasing, stimulated Raman scattering,<sup>1–4</sup> and high sensitivity biological and chemical sensors.<sup>5–13</sup> In the spherical microresonator, the light is confined inside the sphere due to the total internal reflection, as the refractive index of the sphere is larger than that of the surrounding medium. The resonance condition is achieved when the circulating light completes one cycle with in-phase, known as the whispering-gallery-modes (WGMs). Mostly solid dielectric materials are used for making WGMs based microresonators. There are also some reports on the investigation of microresonators based on the isotropic liquids such as CCl<sub>4</sub>,<sup>14</sup> CS<sub>2</sub>,<sup>15</sup> water,<sup>16,17</sup> and glycerol.<sup>18,19</sup> Efforts were also made to prepare polymer<sup>20–26</sup> and single crystal based microresonators.<sup>27–29</sup> However, the tuning of modes in the liquid or solid microresonators is not easy in the sense that their resonance mode frequencies cannot be changed easily. In this context, the recent studies on the microresonators based on nematic liquid crystals are very promising for designing tunable microresonators, which are useful for lasing and biosensors. In this letter, we report studies on the WGM resonance of 8CB liquid crystal droplets with temperature. Our study shows the potential application of WGM resonance of liquid crystal droplets for detecting subtle phase transitions in liquid crystals.

We have used 4-octyl-4'-cyanobiphenyl (8CB) liquid crystal, obtained from Sigma-Aldrich for the experiment. It has the following phase transitions: Cr 21.5 °C, SmA 33.5 °C, and N 40.5 °C. We used 4-dicyanomethylene-2-

methyl-6-(*p*-dimethylaminostyryl)-4H-pyran (DCM) dye as fluorescent material and Polydimethylsiloxane (PDMS) (Sylgard 184, Dow corning) as polymer matrix. In the present experiment no curing agent was added with PDMS. The droplets are prepared in PDMS, which is confined between two glass plates with spacers. The liquid crystal and DCM (<1 wt. %) dye are mixed together to make the microdroplets. The dispersed microdroplets are excited with a tightly focused laser light of wavelength 532 nm (Nd: YAG second harmonic). The absorption peak of DCM matches with the laser wavelength and gives fluorescence in the visible range (540–650 nm). The resonance properties were studied by a scanning near-field optical microscope (WiTec, alpha 200) equipped with a spectrometer. A schematic diagram of the experimental setup is shown in Fig. 1. The evolution of the defect structure was studied as a function of temperature with the help of an optical polarizing microscope (Nikon, LV100 POL). The temperature of the sample was varied by a temperature controller (Instec Inc., mK1000).

We prepared several micron size SmA droplets of 8CB in PDMS by using a micropipette. Typical photomicrographs of a SmA and a nematic microdroplet under optical polarizing microscope are shown in Figs. 2(a) and 2(c), respectively. A sharp spherical boundary with refractive index difference can be seen in Fig. 2(b). Four extinction branches originating from the center and oriented along the polarizer axes suggests that the director distribution is radial and the SmA layers are concentric inside the microcavity. A schematic diagram of concentric SmA layers in the droplet is shown in Fig. 2(d). A point defect is also seen at the centers of the droplets. When the interfacial boundary of dye doped LC microdroplets are illuminated (“+” symbol in Fig. 2(e)) with a tightly focused laser beam ( $\lambda = 532$  nm), a thin light ring along the circumference of the droplet and a brighter spot on the other side of the droplet is seen (Fig. 2(e)). This is due to the excitation of WGMs resonance in the droplet. The fluorescence is observed only inside the droplets suggesting that the dye has not diffused into the surrounding PDMS.

The emitted light is collected with the same objective (20 $\times$ , NA = 0.4) and fed to a spectrometer. The minimum resolution of the spectrometer used for this experiment is

<sup>a)</sup>Present address: Department of Electro-Optic Engineering, Ilse Katz Institute for Nanoscale Science and Technology, Ben-Gurion University of the Negev, Israel

<sup>b)</sup>Electronic mail: sdsp@uohyd.ernet.in

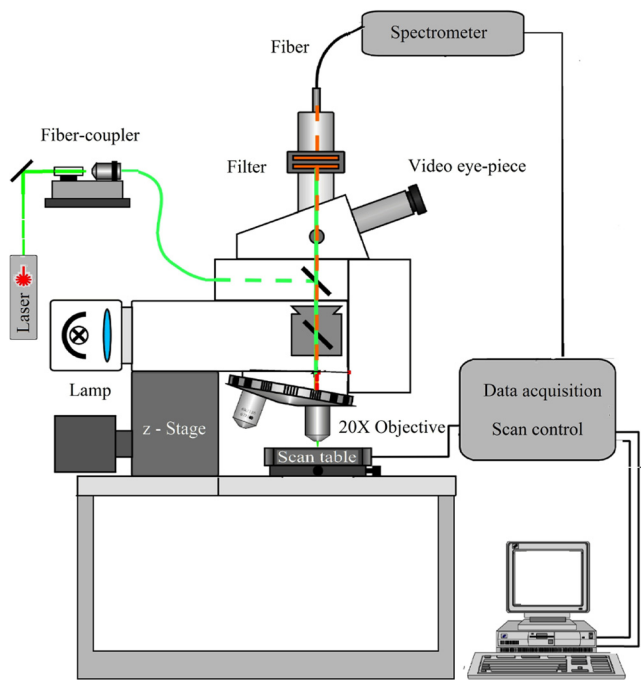


FIG. 1. Schematic diagram of the experimental setup.

limited to 0.09 nm. Usually, the WGMs are characterized by two types of polarizations, namely, transverse electric (TE) and transverse magnetic (TM) modes where the electric field oscillates parallel and perpendicular to the surface of the sphere, respectively. Since LC droplets are birefringent, different polarizations sense different refractive indices. As the droplet exhibits radial structure, the optic axis points in the radial direction. Therefore, the TE mode senses the ordinary ( $n_o$ ) and the TM mode senses the extraordinary ( $n_e$ ) refractive indices. We systematically studied WGMs of LC droplets by varying temperature across the SmA-N phase transition. Figure 3(a) shows the WGM resonances of a 11  $\mu\text{m}$  LC droplet at some representative temperatures. The characteristic resonance spectra from a droplet are observed overlaying the fluorescence background. The line width ( $=\Delta\lambda$ ) corresponding to the resonance peak (at  $\lambda = 600$  nm)

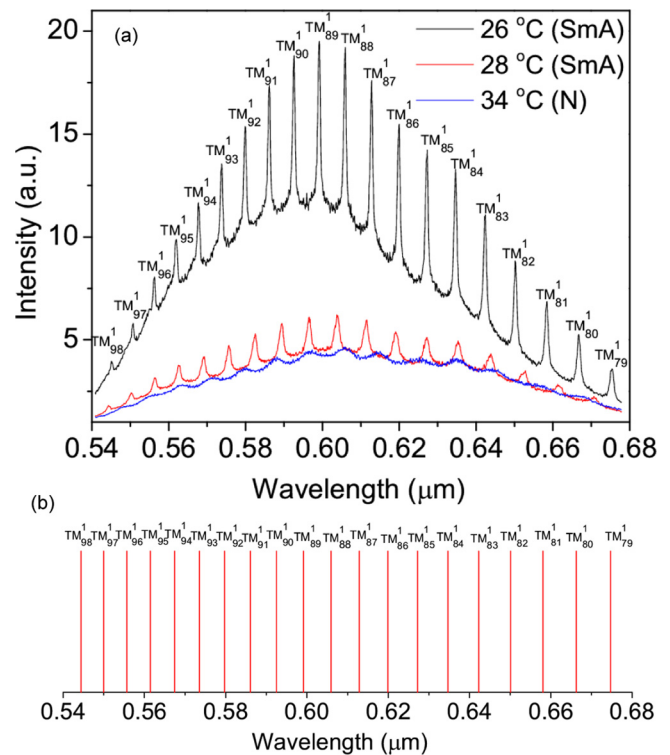


FIG. 3. (a) A set of whispering gallery modes of a liquid crystal droplet at various temperatures. Various mode numbers corresponding with lowest radial modes ( $q=1$ ) with TM polarization. The line width for the  $\text{TM}_{89}^1$  is approximately 0.78 nm, and the LC cavity Q-factor is around 770. The droplet diameter is 11  $\mu\text{m}$ . (b) Simulated resonant frequencies of a LC droplet with corresponding radial mode and TM polarization.

for 26  $^{\circ}\text{C}$  is 0.78 nm and the Q factor ( $\lambda/\Delta\lambda$ ) is  $\simeq 770$ . It is almost one order of magnitude less than that reported previously in room temperature nematic droplets.<sup>30</sup> This is due to our instrumental limitation of minimum spectral resolution, in particular, the spectral resolution of our spectrometer is one order of magnitude less than that used in Ref. 30. As the temperature is increased (28  $^{\circ}\text{C}$ ), the fluorescence background decreases and more importantly the resonance width ( $\Delta\lambda$ ) increases and consequently the Q-factor decreases. A

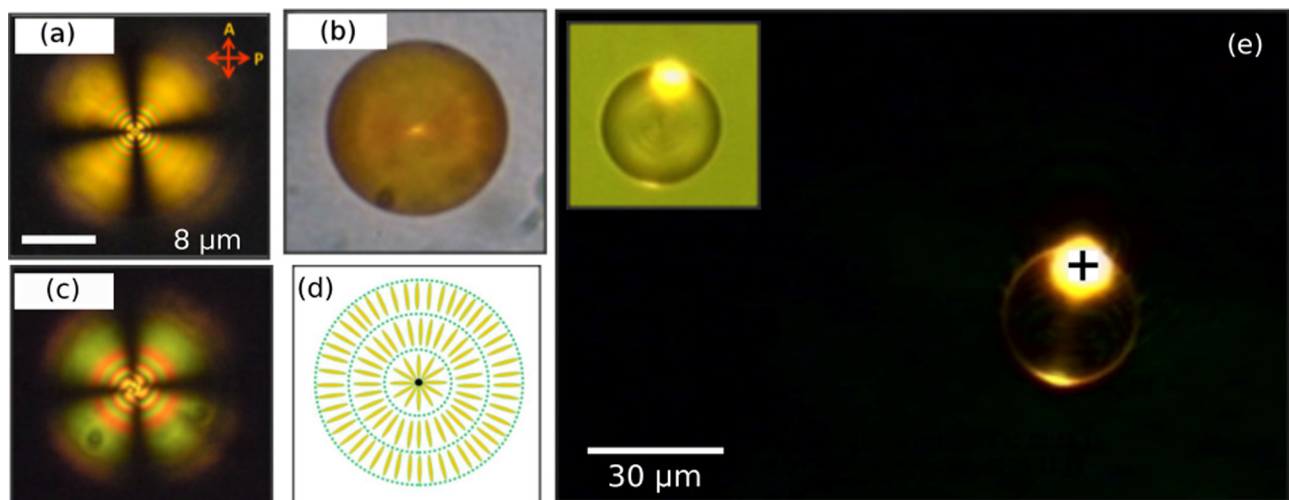


FIG. 2. (a) Photomicrograph of a SmA droplet obtained using optical polarizing microscope. (b) Without polarizers. (c) A nematic droplet between crossed polarizers. (d) Schematic diagram of the SmA layer orientation. (e) Dark-field image of an illuminated SmA droplet. "+" symbol indicates the illumination region with focused laser beam of  $\lambda = 532$  nm. (Inset) Bright-field image of the same SmA droplet.

typical spectra in the nematic phase (34 °C) is also presented in Fig. 3(a). The resonant WGM frequencies for a spherical resonator with small radial mode numbers  $q$  can be simulated using the asymptotic expansion in powers of  $(l/2)^{-1/3}$  (Ref. 31)

$$n_s k a = l - \alpha_q \left(\frac{l}{2}\right)^{1/3} - \frac{\chi n_r}{\sqrt{n_r^2 - 1}} + \frac{3\alpha_q^2}{20} \left(\frac{l}{2}\right)^{-1/3} - \frac{\alpha_q n_r \chi (2\chi^2 - 3n_r^2)}{6(n_r^2 - 1)^{3/2}} \left(\frac{l}{2}\right)^{-2/3} + O(l^{-1}), \quad (1)$$

where  $a$  is the radius of the sphere,  $k$  is the wavenumber,  $l \gg 1$ ,  $q = 1, 2, 3, \dots$  are mode numbers, and  $\chi = 1/n_r^2$  for TM modes.  $\alpha_q$  are negative  $q$ -th zeros of the Airy function, and  $n_r = n_s/n_a$  is the relative refractive index, where  $n_s$  is the refractive index of the sphere and  $n_a$  is the index of the surrounding medium. In the present experiment, for the droplet of diameter 11  $\mu\text{m}$ , we found that only TM modes with radial mode number  $q = 1$  is supported. The experimental resonance peaks for the same droplet are labelled based on the simulated spectra (Fig. 3(b)) using  $n_s = 1.67$ ,<sup>32</sup>  $n_a = 1.37$ .<sup>33</sup> The angular mode numbers  $l$  ranges from 79 to 98.

Figure 4 shows the temperature variation of Q-factor of mode corresponding to  $\lambda = 600$  nm across the SmA-N phase transition. For the sake of comparison, we have plotted with shifted temperature  $T - T_{NS}$ , where  $T_{NS}$  is the SmA-N phase transition temperature. We observe that the Q-factor decreases rapidly with increasing temperature in the SmA phase and tends to saturate in the N phase. For example, it decreases from around 770 to 135 when the temperature is increased from 6 °C below to 4 °C above the transition. We collected the temperature dependence of the birefringence ( $\Delta n = n_e - n_o$ , where  $n_e$  and  $n_o$  refers to the extraordinary and ordinary indices) of the SmA phase from the Ref. 32 and plotted the variation of Q-factor with  $\Delta n$  in the inset of Fig. 4. We found that Q-factor is linearly proportional to  $\Delta n$ . Since  $\Delta n \propto S$ , where  $S$  is the orientational order parameter, the temperature variation of Q-factor truly reflects the

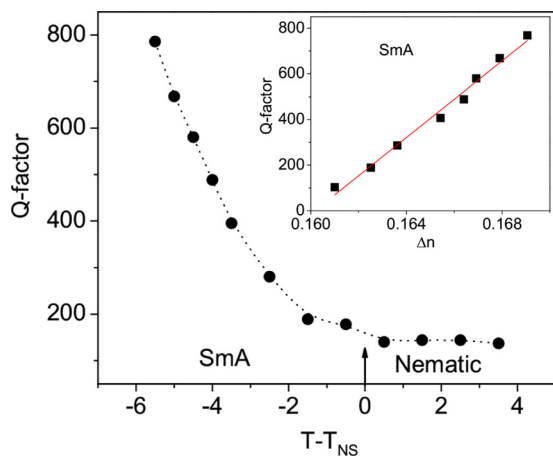


FIG. 4. Temperature ( $T - T_{NS}$ ) variation of Q-factor of the mode corresponding to  $\lambda = 600$  nm. Dotted line is drawn as guides to the eye. The vertical arrow indicates SmA-N phase transition. (Inset) Variation of Q-factor with birefringence ( $\Delta n$ ). The red line is a linear best fit with slope 83850. The droplet diameter is 11  $\mu\text{m}$ .

variation of order parameter. Thus phase transitions among LC mesophases specially the transitions in ferroelectric LCs ( $\text{SmC}^*$ ) subphases namely,  $\text{SmC}_\alpha^*$ ,  $\text{SmC}_\beta^*$ , etc, where the change in  $\Delta n$  is very small could be detected easily by studying the WGM resonances.

Finally, we discuss the possible reason behind the low Q-factor in the nematic phase compared to the SmA phase. Apart from the lower birefringence of the nematic phase, the thermal fluctuations of the director could contribute to the low Q value. In the SmA phase, the director is homeotropic and the layers are concentric (Fig. 2(d)). In the nematic phase the homeotropic boundary condition is retained but in the central region the extinction branches are twisted in the anticlockwise direction (Fig. 2(c)). Similar phenomenon has been observed previously by Lavrentovich and Terent'ev, in other compounds showing SmA to nematic transition.<sup>34</sup> They showed both theoretically and experimentally that radial hedgehog defects in SmA droplets are transformed to hyperbolic hedgehog defects at the SmA-N phase transition keeping the homeotropic boundary condition of the director at the droplet interface. This is due to the critical divergence of the bend elastic constant ( $K_{33}$ ). This transformation is accompanied by a simultaneous formation of nonsingular ring disclination in the nematic phase. A schematic diagram of a singular ring disclination is shown in Fig. 5(a). The transition between them occurs because the core of the droplet surrounded by a nonsingular disclination ring (strength  $m = 1$ ) is leaked away (Fig. 5(b)) and consequently the loss in the cavity increases significantly.

In conclusion, we have studied the whispering gallery mode resonance in 8CB liquid crystal droplets across the SmA to nematic phase transition. We found that the quality factor of the resonance decreases rapidly as the temperature is increased across the SmA-N phase transition. The temperature dependence of Q-factor reflects the temperature dependence of orientational order parameter of the SmA phase. Apart from the director fluctuations in the nematic phase, the energy loss in the nematic phase could partly be due to the change of symmetry of the topological point defect, i.e., from radial hedgehog to hyperbolic hedgehog inside the droplets. The measured Q-factor in the SmA phase is comparatively lower due to the instrumental limitation; nevertheless, the essential features of the WGMs of the droplets

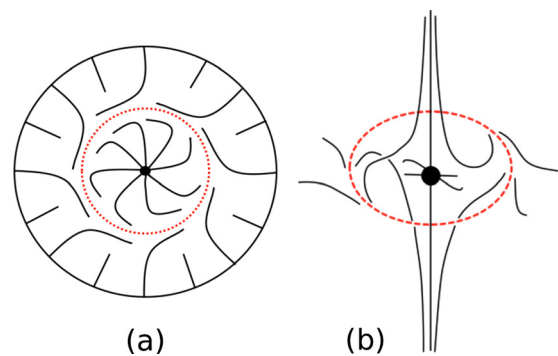


FIG. 5. The schematic diagrams of the director (the average direction of molecular orientation) orientation in a droplet (a) with nonsingular disclination (dotted red line). (b) General appearance with leaked core in the nematic phase.

across the SmA-N transition are revealed. Since the WGMs resonances are very sensitive to the small change in birefringence they can be used for detecting subtle phase transitions such as transitions among the ferroelectric LC subphases.

We gratefully acknowledge support from the DST (SR/NM/NS-134/2010) and CSIR (03(1207)/12/EMR-II), DST PURSE, and UPE-II. We also acknowledge the facilities of Center for Nanotechnology.

- <sup>1</sup>K. Vahala, *Optical Microcavities* (World Scientific, 2004).
- <sup>2</sup>S. Arnold, S. Holler, and S. D. Druger, "Optical processes in microcavities," edited by R. K. Chang and A. J. Campillo, in *Advanced Series in Applied Physics* (World Scientific, Singapore, 1996), Vol. 3.
- <sup>3</sup>A. B. Matsko and V. S. Ilchenko, *Quantum Electron.* **12**, 3 (2006).
- <sup>4</sup>V. S. Ilchenko and A. B. Matsko, *Quantum Electron.* **12**, 15 (2006).
- <sup>5</sup>F. Vollmer and S. Arnold, *Nat. Methods* **5**, 591 (2008).
- <sup>6</sup>S. Arnold, S. I. Shopova, and S. Holler, *Opt. Express* **18**, 281 (2010).
- <sup>7</sup>X. Fan, I. M. White, S. I. Shopova, H. Zhu, J. D. Suter, and Y. Sun, *Anal. Chim. Acta* **620**, 8 (2008).
- <sup>8</sup>S. Arnold, M. Khoshshima, I. Teraoka, S. Holler, and F. Vollmer, *Opt. Lett.* **28**, 272 (2003).
- <sup>9</sup>F. Vollmer, S. Arnold, and D. Keng, *Proc. Natl. Acad. Sci. USA* **105**, 20701 (2008).
- <sup>10</sup>M. Loncar, *Nat. Photonics* **1**, 565 (2007).
- <sup>11</sup>H. Wang, L. Yuan, C-W. Kim, Q. Han, T. Wei, X. Lan, and H. Xiao, *Opt. Lett.* **37**, 94 (2012).
- <sup>12</sup>J. J. Yang, M. Huang, X. Z. Dai, M. Y. Huang, and Y. Liang, *Europhys. Lett.* **103**, 44001 (2013).
- <sup>13</sup>L. He, S. K. Ozdemir, J. Zhu, W. Kim, and L. Yang, *Nat. Nanotechnol.* **6**, 428 (2011).
- <sup>14</sup>H. B. Lin and A. J. Campillo, *Phys. Rev. Lett.* **73**, 2440 (1994).
- <sup>15</sup>R. G. Pinnick, A. Biswas, P. Chylek, R. L. Armstrong, H. Latifi, E. Creegan, V. Srivastava, M. Jarzembki, and G. Fernandez, *Opt. Lett.* **13**, 494 (1988).
- <sup>16</sup>R. J. Hopkins, R. Symes, R. M. Sayer, and J. P. Reid, *Chem. Phys. Lett.* **380**, 665 (2003).
- <sup>17</sup>S. X. Qian, J. B. Snow, H. M. Tzeng, and R. K. Chang, *Science* **231**, 486 (1986).
- <sup>18</sup>A. Biswas, H. Latifi, R. L. Armstrong, and R. G. Pinnick, *Phys. Rev. A* **40**, 7413 (1989).
- <sup>19</sup>A. Kiraz, M. A. Dundar, A. L. Demirel, S. Doganay, A. Kurt, A. Sennaroglu, and M. Y. Yuce, *J. Nanophotonics* **1**, 011655 (2007).
- <sup>20</sup>M. Kuwata-Gonokami, R. H. Jordan, A. Dodabalapur, H. E. Katz, M. L. Schilling, R. E. Slusher, and S. Ozawa, *Opt. Lett.* **20**, 2093 (1995).
- <sup>21</sup>M. Kuwata-Gonokami and K. Takeda, *Opt. Mater.* **9**, 12 (1998).
- <sup>22</sup>P. Rabiei, W. H. Steier, C. Zhang, and L. R. Dalton, *J. Lightwave Technol.* **20**, 1968 (2002).
- <sup>23</sup>G. T. Paloczi, Y. Huang, and A. Yariv, *Electron. Lett.* **39**, 1650 (2003).
- <sup>24</sup>S. Ashkenazi, C.-Y. Chao, L. J. Guo, and M. O. Donnell, *Appl. Phys. Lett.* **85**, 5418 (2004).
- <sup>25</sup>V. D. Ta, R. Chen, and H. D. Sun, *Sci. Rep.* **3**, 1362 (2013).
- <sup>26</sup>M. Saito, H. Shimatani, and H. Naruhashi, *Opt. Express* **16**, 11915 (2008).
- <sup>27</sup>V. B. Damiao, E. Fotheringham, V. Shkunov, L. Czaia, and D. Z. Anderson, *Opt. Lett.* **26**, 611 (2001).
- <sup>28</sup>A. A. Savchenkov, V. S. Ilchenko, A. B. Matsko, and L. Maleki, *Phys. Rev. A* **70**, 051804 (2004).
- <sup>29</sup>V. S. Ilchenko, A. B. Matsko, A. A. Savchenkov, and L. Maleki, *Proc. SPIE* **4629**, 158 (2002).
- <sup>30</sup>M. Humar, M. Ravnik, S. Pajk, and I. Musevic, *Nat. Photonics* **3**, 595–600 (2009).
- <sup>31</sup>C. C. Lam, P. T. Leung, and K. Young, *J. Opt. Soc. Am. B* **9**, 1585 (1992).
- <sup>32</sup>R. G. Horn, *J. de Physique* **39**, 105 (1978).
- <sup>33</sup>Matjaz Humar, Ph.D. dissertation (Jozef Stefan International Post Graduate School, Ljubljana, 2012).
- <sup>34</sup>O. D. Lavrentovich and E. M. Terent'ev, *Sov. Phys. JETP.* **64**, 1237 (1986).